

Groundwater Potential Evaluation and Aquifer Characterization using Direct Current Resistivity Method in Wasinmi South-West Nigeria



*¹Ishola, S. A. and ²Bukar, M.

¹Department of Earth Sciences, Olabisi Onabanjo University Ago-Iwoye, P.M.B 2002, Ago-Iwoye, Ogun State, Nigeria

²Department of Geology, University of Maiduguri, Borno State, Nigeria

*Corresponding author's email: ishola.sakirudeen@oouagoiwoye.edu.ng

ABSTRACT

The effectiveness in near-surface characterization makes geoelectrical resistivity techniques viable for groundwater exploration, geotechnical studies and environmental investigations. Geo-electric soundings were carried out in 25 different locations in Wasinmi, South-West Nigeria to acquire aquifer properties required for groundwater production of the study area using Direct Current Resistivity (DCRE) of Vertical Electrical Sounding (VES) utilizing AGI Super-sting Earth Resistivity meter with schlumberger configuration; current electrode spacing (AB) ranging from 1 to maximum of 100 m and the potential electrodes (MN) were consequently changed from 0.25 m to 5 m respectively. The simulated results of the 25 VES points reveal the presence of 3 to 4 geo-electric layers. The top layer comprises clay, sand, siltstone intercalations. Layers underneath the top soil are the Lithified Laterite, Clayey Sand, Clay/Shale, Sandy Clay and Limestone/Sandstone, Saturated, Sandstone Aquifer. The area is also characterized with relatively high depth to sandstone aquifer which varies from 20 m to 69.1 m. This can be attributed to the thick water saturated Shale/Clay and Clayey Sand in the area. However, at the extreme of North-Western part of the study area, depths to aquifer are far lower, with VES location VESWAS15 having a thickness of about 14.4 m. Aquifer thickness in the study area varied from 14.4m to 63.5m. VESWAS19 has the highest aquifer resistivity value (2473 Ω m) in the study area, with depth to aquifer of 69.1 m. The transmissivity varies between $0.17695 \times 10^{-5} m^2/s$ in VESWAS4 to $8.97654 \times 10^{-5} m^2/s$ in VESWAS13. This study further shows that aquifer resistivity values vary from 284 Ω m to 2473 Ω m with a range of 2189 with the resistivity values suggesting lithology in the suite of Sandy Clay, Sandstone and Karst Limestone found to be widespread in the study area with mean aquifer thickness value of 32.25 m and a variance of 124.63 m. The utilization of Direct Current Resistivity survey permitted us to locate the best places to drill wells and to install boreholes for effective tapping of freshwater resources in the study area.

Keywords:

Aquifer Resistivity,
Geo-Electric Layer,
Geo-Electric Soundings,
Transmissivity.

INTRODUCTION

The quest for good quality water to sustain human lives and other biological population has caused a reasonable drift from ordinary search for surface water to prospecting, exploring and exploitation of sub-surface groundwater for steady and reliable supply in Wasinmi area of Ogun State, Southwest Nigeria. Electrical resistivity method is one of the most useful techniques in groundwater geophysical exploration, because the resistivity of rocks is sensitive to its ionic content (Alile *et al.*, 2011). The method allows a quantitative result to

be obtained by using a controlled source of specific dimensions. Records show that the depths of aquifers differ from place to place because of variation in geo-thermal and geo-structural occurrence (Okwueze, 1996). Available boreholes may fail to sustain regular water supplies, because of the complex subsurface geology (Okereke, *et al.*, 1998; Ishola *et al.*, 2021); therefore, the need to investigate groundwater production. The study area lies within $6^{\circ}58'0''$ N and $3^{\circ}28'60''$ E in DMS (Degrees Minutes Seconds) or 6.96667 and 3.48333 (in decimal degree) with a population amounts of 536,068

(NPC, 2014). The overall objective of the research is to detect groundwater potential and provide data for the development of boreholes in the area. The study derived the resistivity of the sub-surface geologic boundaries from their conductivities and used same to determine geo-electrical parameters and establish the geo-electric sections, delineate the thickness of aquifer units and evaluate the aquifer parameters in order to access groundwater potentials of the area. This study characterized the aquifer dimensions in the area, for substantial groundwater development at any particular point in time. The contour maps of aquifer properties including aquifer resistivity and aquifer transmissivity which permit the swift assessment of aquifer characteristics were also undertaken.

Study Area

Location, Geology and Hydrology of the study Area

Wasimi is located in parts of Dahomey basin in Ewekoro Local Government Area of Ogun State at an elevation of 79 metres above sea level with coordinates of 6°58'0" N and 3°28'60" E in DMS (Degrees Minutes Seconds) or 6.96667 and 3.48333 (in decimal degree) and its population amounts to 536,068. The history of the people reveals that culture and tradition play a central role in their indigenous beliefs system. The neighborhood include Ogun state sport academy, an under construction industrial factory site, the proposed Ogun State Cargo, international airport in Wasinmi and so on (Ishola, 2019).

Over fifty percent of the land area of southwestern Nigeria lies within the coastal plain where the relief is generally low with average elevation of about 200 m – 400 m above sea level (Jones and Hockey, 1964). Three major landform units, namely the hills, plains and river valleys, dominate the study area. The hills are the most striking feature, although they constitute less than 30 % of the total surface area. The plains are the most striking landform system in the investigated areas (with an average elevation of 64m above sea level) which ranges between 46 m and 107 m in Wasinmi. The river valleys are the narrowest landform in the area. The rivers in the study area display are in form of sluggish perennial streams in dry season but are turbulent during the wet season. This relief can be described as undulating and the drainage is dendritic (Okosun, 1998; Ishola, 2019; Ishola et al., 2021).

Ewekoro formation is the local geology in the study area which is generally consistent with the regional geology of eastern part of the Dahomey Basin; predominantly comprises of the non-crystalline and highly non-fossiliferous limestone and thinly laminated fissile and probably non-fossiliferous shale (Adegoke, 1969; Ushie et al., 2014; Ogbe, 1972). Ewekoro formation consists of intercalations of argillaceous sediment. The rock is soft and friable but in some places cement by

ferruginous and siliceous materials. The lithological units in Ewekoro formation are clayey sand, clay, shale, marl, limestone and sandstone. The lithology of Ise and Afowo formations as defined by Omatshola and Adegoke (1981) show a high degree of similarity. Both are essentially sands and sandstones, but the latter contains thick interbeds of shales. This difference is not sufficient to warrant the establishment of separate lithostratigraphic units. The two formations were considered synonymous by Okosun (1998). In that study, it was observed that the Ise, Afowo and Abeokuta formations have similar lithologic and electric log characters. The uppermost beds of Abeokuta formation which crop out in Ijebu Ode area and in the shallow boreholes at Itori, Wasimi and Ishaga onshore consist mainly of fine to coarse grained sand and interbeds of shale, mudstone, limestone and silt. These lithofacies correlate well with the upper portion of the neostatotype in Ojo-1 borehole Okosun (1998). The Abeokuta formation was defined by Jones and Hockey (1964) to consist of grits, loose sands, sandstones, kaolinic clay and shale and was further characterized as usually having a basal conglomerate or basal ferruginized sandstone. The Abeokuta formation on surface outcrops comprises mainly sand with sandstone, siltstone, silt, clay, mudstone and shale interbeds. It usually has a basal conglomerate which may measure about 1m in thickness and usually consists of poorly rounded quartz pebbles with silicified and ferruginized sandstone matrix or a softly gritty white clay matrix. In outcrops where there is no conglomerate, a coarse, poorly sorted pebbly sandstone with abundant white clay constitutes the basal bed. The overlying sands are coarse grained clayey, micaceous and poorly sorted and indicative of short distances of transportation or short duration of weathering and possible derivation from the granitic rocks located to the north. Subsurface data on the Abeokuta formation was obtained from Ise-2, Afowo-1, Orimedu-1, Bodashe, Ileppawi, Ojo-1 and Itori boreholes by Okosun (1990). The formation has a thickness of 849 m, 898 m, 624 m, 54.4 m and 888 m in Ise-2, Afowo-1, Ileppawi, Itori and Ojo-1 boreholes respectively. In the Ise-2 borehole, the essentially arenaceous sequence between 1261.5 m and 2142.1 m which consists of sands, grits, sandstone, siltstone, clay and shale constitutes the formation (Archibong, 1978; Oyedele and Adeyemo, 2001; Ishola et al., 2021). The interval 1076 m – 1907 m which is made up of very coarse loose sands with sporadic thin intercalations of multicoloured shale and limestone represents the formation in Ojo-1 borehole. The strata from the 44 m to 98.4 m in the Itori borehole, which consists of coarse-fine and medium-grained sand, silt and sandy clay horizons, constitutes the upper portion of the formation. The Ise-2 borehole also penetrated a basal conglomerate. Jones and Hockey (1964) revealed

Ewekoro limestone and the overlying Akinbo shale to be lateral equivalents of the Imo formation of eastern Nigeria. Other authors such as Omatsola and Adegoke (1991) and Oladeji (1992) have investigated the stratigraphy and depositional characteristics of limestone and clay/shale deposits in south-western Nigeria. The West African Portland Cement Company also conducted extensive geological survey and commercial appraisal of Ewekoro limestone and shale beds for commercial cement production. Although the water bearing rocks in large quantity are the sedimentary rocks, the basement rocks which underlies the area though hydrogeologically problematic appears to present relatively good ground water potential thought to be the reliable aquifers for small scale village, institution, industries and other water supply schemes. Offodile (1983) explained that the crystalline rocks are poor ground water regions with recorded

average yield of 3960 liters /hrs (880 gph) at average depth of 37.3 m (123 ft) and over 30 % failure rate in water borehole drilling. Previous work shows that sedimentary aquifers give higher groundwater yield than the basement complex aquifer. Jones and Hockey (1964) evaluates depth, yield and specific capacity of tube wells which tap the Abeokuta formation, Ewekoro formation (Dahomey Basin) and coastal Plain sands with recent alluvium, in the Niger delta complex.

Fig. 1 shows the Geology map showing the study area in South-West Nigerian part of Dahomey Embayment, Fig. 2 is the geology map of the entire Sedimentary basins of Nigeria, Figure. 3 is an inset map which reveals the study area in Ogun State within continental Domain of South-West Nigeria while Fig. 4 is the data acquisition map which shows the investigated locations in Wasinmi study area within Ewekoro Local Government area of Ogun state, South-West, Nigeria.

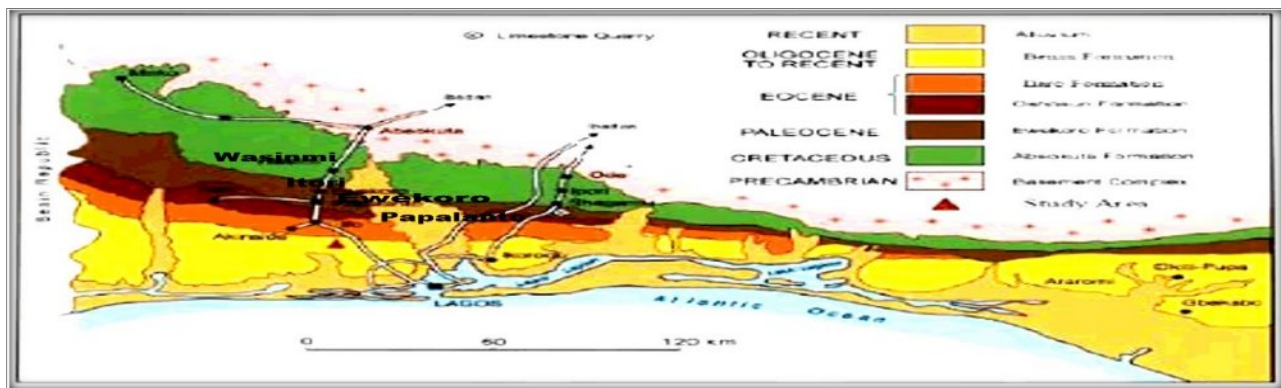


Figure 1: Geological Map Showing the Study Area within the South-West Nigerian Part of Dahomey Embayment (Billman, 1992; modified by Ishola, 2019).

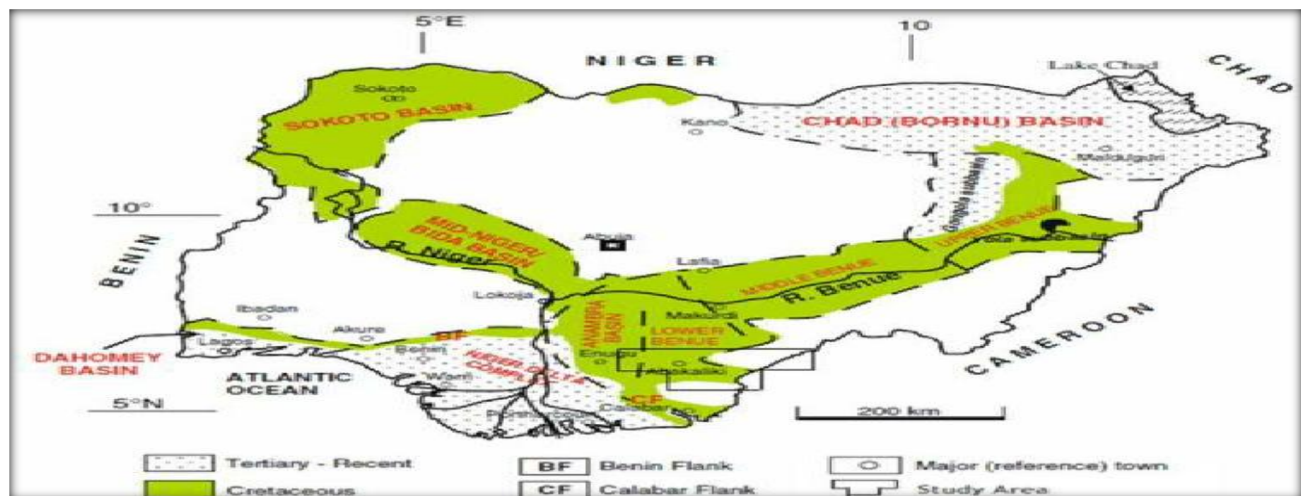


Figure 2: Map of the entire sedimentary basin of Nigeria showing the study area as part of Dahomey embayment (After, Obaje 2009; modified by Ishola, 2019)

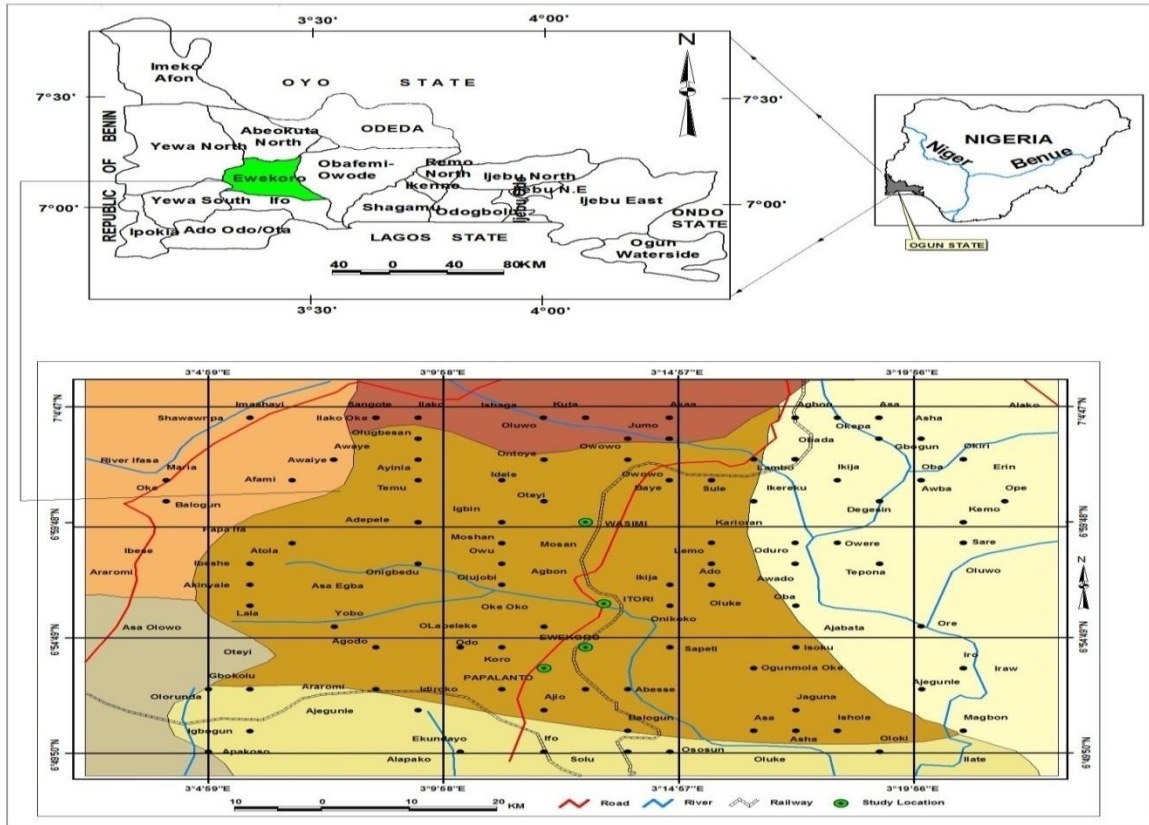


Figure 3: Inset Map showing the Study Areas in Ogun State within Nigeria Continental Domain (Ishola, 2019)

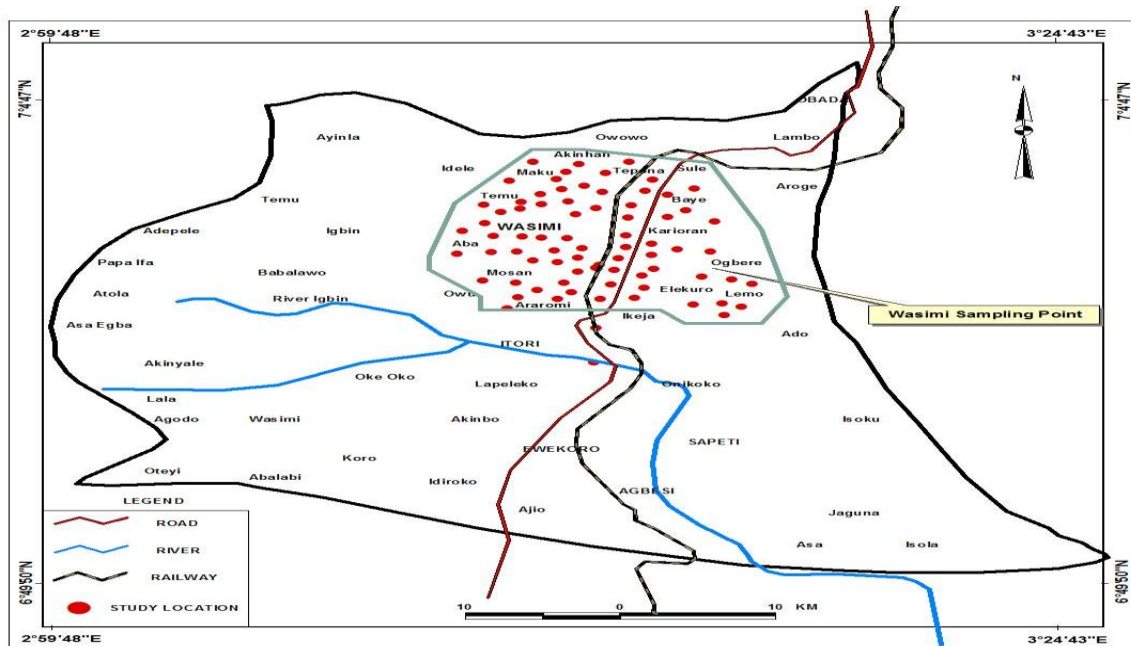


Figure 4: Data Acquisition Map showing the Investigated Locations in Wasimi Study Area within Ewekoro LGA, Southwest Nigeria (Ishola, 2019).

MATERIAL AND METHODS

Vertical Electrical Sounding (VES) using Schlumberger configurations was adopted. The basic field equipment used for the study is Super Sting Earth Resistivity meter which was used to measure the apparent resistance that the ground offers to the flow of electric current through it and display apparent resistivity value digitally as computed from Ohm's law (Ishola *et al.*, 2021). It performs automatic recording of both voltage and current, stacks the results, computes the resistance in real time and digitally displays it on its screen. The electrode arrangement used in data acquisition is the Schlumberger array of electrodes. Soundings were performed at 25 locations with maximum current electrodes separation ranging between 100 m and 200 m.

The terrameter is powered by 12V D.C power source. Other materials that accompany the equipment are

measuring tape, 4 hammers, 45 metal electrodes where 4 metal electrodes were used. The four electrodes are positioned symmetrically along a straight line, the current electrodes on the outside and the potential electrodes on the inside. To change the depth range of the measurements, the current electrodes are displaced outwards while the potential electrodes in general, are left at the same position (Goes and Meekes, 2004). When the ratio of the distance between the current electrodes to that between the potential electrodes becomes too large, the potential electrodes must also be displaced outwards otherwise the potential difference becomes too small to be measured with sufficient accuracy (Koefoed, 1979; Alile, 2008). Measurements of current and potential electrode positions are marked such that $AB/2 \geq MN/2$ (Figure. 5).

where $AB/2 =$ Current electrode spacing and $MN/2 =$ Potential electrode spacing.

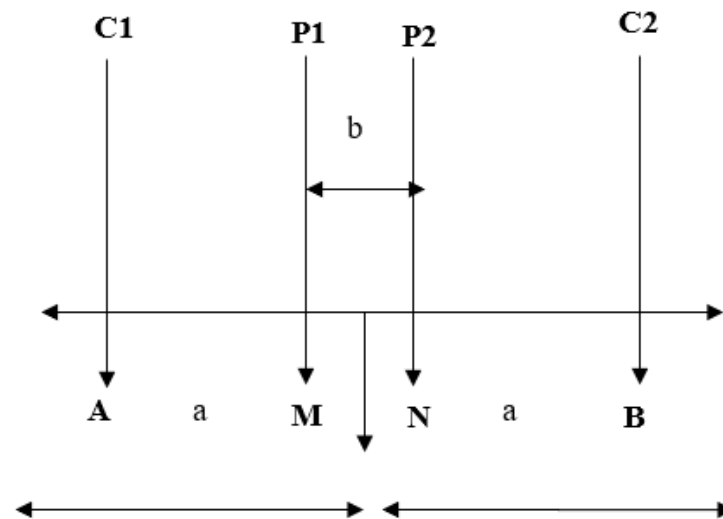


Figure 5: Schlumberger Electrode Configuration on the Field

Generally, the arrangement consists of a pair of current electrodes and a pair of potential electrodes. These are driven into the earth in a straight line to make a good contact with the earth. The current electrode spacing is expanded over a range of values for measurements in the field. The value of $AB/2$ increases as the measurements progresses, the potential electrodes separations are guided accordingly. The potential electrodes are kept at small separations relative to the current electrodes separations (Alile, 2008; Ishola *et al.*, 2021). One of the major advantages this method has over other methods is that only the current electrodes need to be shifted to new position for most readings while potential electrodes are kept constant for up to three or four readings (Dobrin, 1985; Alile, 2008). During the field work taking a sounding, the earth resistivity meter performs automatic recording of both

voltage and current, stacks the results, computes the resistance in real time which it multiplies with the geometrical factor (a function of the distance within the current and potential electrodes) to give the resistivity and digitally displays the Apparent Resistivity (Dobrin, 1985; Mamah and Eze, 1988; Alile, 2008; Ariyo *et al.*, 2009; Ishola *et al.*, 2021).

Field procedures

The field work was carried out between January and February, 2017 close to the peak of of dry season when the ground was considerably moist. This ensured good current conduction between the earth and the electrodes. The data collection was performed by a five-man crew which included the research reporter. Two men were positioned at the centre of the spread: the researcher who was controlling the instrument, adjusting readings

and recording the data from the meter and monitors through the meter's display, when electrical contact was poorly established or otherwise. The Terrameter usually displays negative resistance when signal current to the ground is insufficient. At such stages the instrument observer adjusts to high current signals. The second person at the centre of the spread adjusts the potential electrodes when necessary and communicates to the rear men when to take the necessary steps of the observational procedures. This was usually done during looping. At looping stage, different resistance readings were taken at the same current electrode separation. The essence of looping is to permit the detection of near surface in-homogeneities and establish communication contact between the instrument controller and the two rear men especially when they are very far from spread centre. The rear-men are responsible for maintaining the current electrode spacing, moving and driving the current electrodes into the ground; a quick on the spot inspection was carried out to decide where to run the traverse line. Since high conductivity often correlates with deeply weathered materials, fractures or conductive bodies which is often the target in hydro-geophysical investigation (Olayinka, 1990), where identified were priority areas for depth sounding. This is because electrical resistivity is cheap and has a relatively high diagnostic value (Ariyo *et al.*, 2009) and can furnish information on subsurface geology (Nur and Kujir, 2006), without the large cost of an extensive programme of drilling (Kearey and Brooks, 1991). Though, there are many electrode arrays that could be used in resistivity survey, viz- Wenner array, Schlumberger array, pole dipole array and double dipole array, the Schlumberger electrode configuration was employed for the vertical electrical sounding conducted in the study area because, its field operation is easy. The maximum current electrode separation (AB) was 400m although much later shorter electrode separations could prove adequate for getting the high resistive values characteristic of sedimentary formation. The potential electrodes were expanded symmetrically about a fixed centre of spread (Parasins, 1986, Kearey and Brooks, 1991). A total of twenty five (25) vertical electrical sounding points were carried out at each at each study area.

The observed field data was converted to apparent resistivity by multiplying with the Schlumberger geometric factor. The geometric factor for the Schlumberger array is given by:

$$G = \frac{\pi}{2l} [L^2 - l^2] \quad (1)$$

where L= half current electrode spacing and l = half potential electrode spacing

The apparent resistivity data were plotted against the half current electrode spacing in meters in)the

horizontal axis. The resistivity data were further interpreted using IPI2Win inversion software package (Bobachev, 2002). The curves resulting from the plots of some of the VES points are given in figure 2.1 while the summary of results of the aquifer parameters integrated from the geo-electric sections in the study area is presented in Table 1.

Singh (2005) established a non-linear relationship between hydraulic conductivity (K) and apparent resistivity (ρ) given by

$$K = 0.0538e^{-0.0072\rho} \quad (\text{Singh, 2005}) \quad (2)$$

where ρ equals the apparent resistivity of the formation, (Abdullahi, *et al.*, 2011)

$$T = Kb \quad (\text{Ekwe, et al., 2006}) \quad (3)$$

where T = Transmissivity (m²/sec) and b = Aquifer Thicknesses.

RESULT AND DISCUSSION

Resistivity Sounding Curves

The resistivity sounding curves obtained from the surveyed area was a typical 4 layer (H type), with few 5-layer (KH) as shown in Figure 6. The H-type curve with about 84.2% of occurrence and KH-type curve with about 15.8% of occurrence were deduced from the area (Figure. 6). Worthington (1977) showed that field curves often mirror image geoelectrically revealing the nature of the successive lithologic sequence in an area and hence can be used qualitatively to assess the groundwater prospects of an area. The H and KH curves which are often associated with groundwater possibilities (Omosuyi, 2010) are pertinent to the study area. The geo-electric parameters of the lithologic units shown in Table 1 were delineated from the interpreted sounding curves shown in Figure 6. since Electrical resistivity methods primarily reflect variations in ground resistivity (Omosuyi *et al.*, 2008; Oyedele and Adeyemo, 2001 and Okafor and Mamah, 2012; Ishola *et al.*, 2021).

Statistical Analysis of Aquifer Parameters

Descriptive Statistical Analyses of the geoelectrical parameters was carried out on the VES data acquired from 25 selected study locations within Wasinmi in Ewekoro Local Government Area of Ogun State, Southwestern Nigeria. Basic parameters analyzed include Resistivity of Top Soil, Thickness of Top Soil, Aquifer Resistivity, Aquifer Thickness, Bedrock Resistivity, Bedrock Relief, Overburden Thickness, Longitudinal Unit Conductance, Coefficient of Anisotropy, Transmissivity and Hydraulic Conductivity. The summary of the Aquifer Parameters of the study area are shown in Table 1 while the summarized results of the Statistical Analyses of the acquired parameters using SPSS Version 20.0 Statistical software are hereby presented in Table 2.

The Topsoil resistivity values vary from 81.20 Ωm to 645 Ωm with a range of 563.80. The high range and variance of topsoil resistivity values observed suggests dissimilarities in the mineralogical composition of the geologic materials constituting the top soil (Ishola, 2019). The aquifer resistivity values vary from 284 Ωm to 2473 Ωm with a range of 2189. This range of aquifer resistivity values obtained in correlation with the hydrogeologic materials of the study area determines to a significant extent the yield of boreholes as well as its water qualities (Burger, 1992). The resistivity suggests lithology in the suite of Sandy Clay, Sandstone and Karst Limestone to be widespread. The mean aquifer thickness value is 32.25 m with a variance of 124.63 m (Table 2). Hydrogeologically, the weathered layer is highly relevant in groundwater prospecting when it is thick enough, above minimum thickness of 10 m suggested by Walter *et al.*, (1981), the layer could appreciably support hand-dug well (Olorunfemi and Okhue, 1992). In these study areas the recorded thickness values are relatively high and measures the degree of the clustering of the data around the mean. From the obtained results, it was shown that very few locations exhibits low bedrock resistivity values less than 1000 Ωm in all the study areas which suggests lithology in the suite of Sandstone, Saturated Sandstone and Fractured or Weathered Limestone. Therefore, it could be stated that areas with low bedrock resistivities as well as low bedrock reliefs are the areas of appreciable prospects in terms of groundwater abstraction (Ishola *et al.*, 2016). A range of value of longitudinal conductance value of 0.04 with an average value of 0.02 Siemens was recorded (Table 2). Telford *et al.*, (1976) stated that, the conductance is related to clay content which increases the porosity of its layer but decreases its permeability. Since permeability decreases with an increase in conductance, the overburden might therefore have absorption and retention capacity. Wasinmi has a mean overburden thickness value of 27.73 m with a range of 65 m. The above overburden thickness values depict the depth to the aquiferous zones and it can be used to assess the cost effectiveness of the area in terms of the amount/cost of drilling as well as the efficiency (Coker *et al.*, 2009; Ishola *et al.*, 2016). In terms of Coefficient of Anisotropy, Wasinmi has a standard deviation value of 0.00005 with a mean value of 1.000 with a null range (Table 2). Generally, the Coefficient of Anisotropy (λ) is 1 and does not exceed 2 in most of the geological conditions (Zohdy *et al.*, 1974). Compact rock at shallow depth increases the coefficient of Anisotropy (Keller and Friscknecht, 1966). More than 2 coefficient of Anisotropy value (λ) indicates very hard Porphyritic Granite Gneiss and Garnet Biotite Gneiss terrain of the geological environment while areas that are less than 1.5 Coefficients of Anisotropy values are considered as

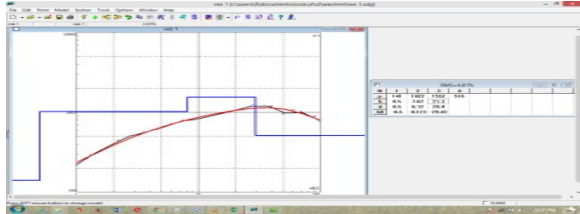
potential aquifers for groundwater abstraction and prospecting. Alluvial aquifers, fractured zones and valley fills with anisotropy value around 1.00 are recognized as good groundwater potential zones. These results are evidences that the hydrogeological environment of the investigated area is typically a sedimentary formation with exhibited layered structures. It is noteworthy that in all the study areas, Coefficient of Anisotropy is negatively skewed with low values of Standard deviation (SD) and generally zeros recorded variance depicting a low degree of distortion or disparity to the normal value (Ishola *et al.*, 2016; Ishola, 2019).

Transmissivity is the rate at which water flows through a vertical strip of the aquifer of unit width and extending to full saturated thickness under hydraulic gradient 1.00. Using $T = Kh$ where K is the coefficient of conductivity (m/s), h is the aquifer thickness(m), the estimates of T obtained in the study areas shows that Wasinmi exhibited the value range of $9.0 \times 10^{-5} \text{ m}^2/\text{s}$ with a mean value of $2.0 \times 10^{-5} \text{ m}^2/\text{s}$ with a relatively low recorded standard deviations. It is positively skewed with values of 0.24 ± 0.46 . The weathered nature of the consolidated sedimentary rock formation may be responsible for the observed transmissivity values in all the study areas (Coker *et al.*, 2009; Ishola *et al.*, 2016; Ishola, 2019). In the Hydraulic Conductivity (K) parameter, using the relation $K = 95.5 \times 10^{-9} \rho^{1.195}$ where ρ is the resistivity of the porous layer in Ohm-m (Mazae *et al.*, 1985), near zero to zero variation of conductivity values were observed in the study area from aquifer to aquifer. A range of $1.0 \times 10^{-2} \text{ m/s}$ with a mean value of $3.0 \times 10^{-4} \text{ m/s}$ was recorded. In general, these recorded values are relatively low in all the study areas. The low values recorded could be attributed to probably the overlying and intercalations of clay materials in the aquifers. K is positively skewed in the study area with a value of 4.99 ± 0.46 which signifies a low departure from the symmetry (Ishola *et al.*, 2016; Ishola, 2019). The degrees of scattering are equally very small with a very low standard deviation of 0.038. The applied descriptive statistics using Skewness and Kurtosis describe the resultant shape of the aquifer parameters distribution in all the investigated area. Skewness is a measure of symmetry or relative sizes of the distribution. Whenever the skewness value is 0, positive or negative reveals the shape of the data. As the data becomes more symmetrical; its skewness value approaches 0. Normally distributed data exhibits relatively little skewness. Positive skewed data or right skewed data is so named because the 'tail' of the distribution points to the right and its skewness value will be greater than 0 or positive while a negative skewed data is so named because the 'tail' of the distribution points to the left, and it produces a negative skewness value (Table 2).

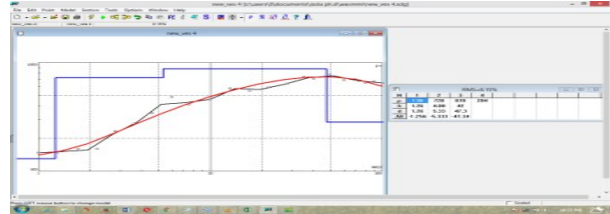
Kurtosis is a measure of combined weight of the tails relative to the rest of the distribution. It measures the amount of the probability in the tails. Kurtosis elucidates the initial understanding of the general characteristics about the distribution of data as it indicates how the peak and tails of a distribution differ from the normal distribution. The baseline is data that follow a normal distribution perfectly have a kurtosis value of 0. Normally distributed data establishes the baseline as sample values that deviate from 0 may

indicate that the data are not normally distributed. A distribution with a positive kurtosis value indicates that the distribution has heavier tails and a sharper peak than normal distribution while a distribution with negative kurtosis value indicates that the distribution has lighter tails and a flatter peak than the normal distribution. If the Kurtosis is greater than 3, then the dataset has a heavier tails than a normal distribution. If the Kurtosis is less than 3, then the dataset has lighter tails than a normal distribution (Ishola *et al.*, 2016; Ishola, 2019).

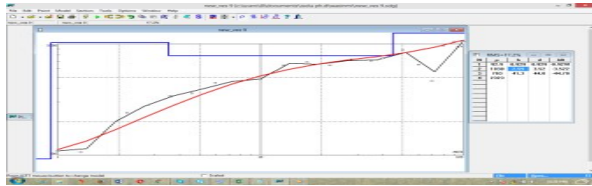
VESWAS1



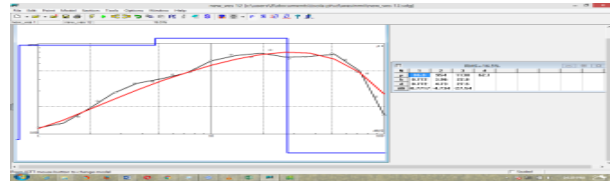
VESWAS4



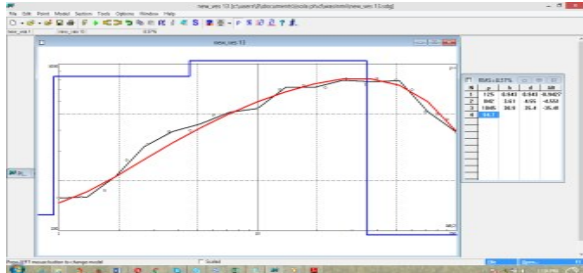
VESWAS9



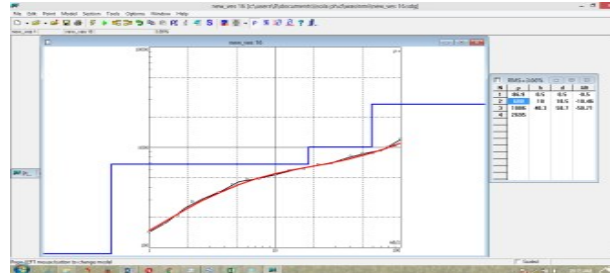
VESWAS12



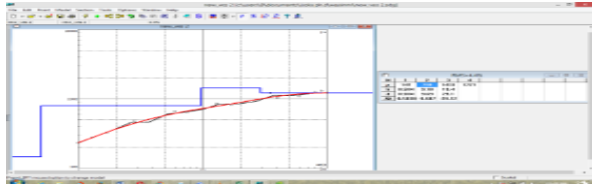
VESWAS13



VESWAS16



VESWAS21



VESWAS25

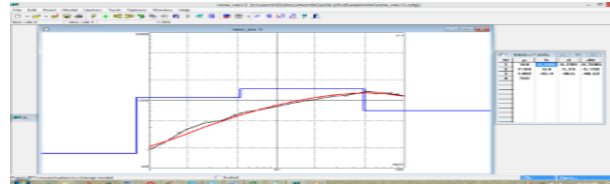


Figure 6: Typical VES curves representing investigated sounding points in Wasinmi (Ishola, 2019).

Table 1: Summary of Results of the Aquifer Parameters

Ves Stations	Aquifer Resistivity ρ_a (Ωm)	Aquifer Thickness (m)	Depth to Aquifer (m)	Overburden Thickness (m)	Longit Conductance (S)	Hydraulic Conductivity (m/s)	Transmissivity (m^2s)	Inferred Lithology
VESWAS1	1552	21.3	29.4	29.4	0.009106	7.54748×10^{-7}	1.60761×10^{-5}	Limestone/Sandstone
VESWAS2	1433	19.4	29.1	29.1	0.008078	1.77789×10^{-6}	3.44913×10^{-5}	Limestone/Sandstone
VESWAS3	1964	32.5	46.8	46.8	0.012503	3.32104×10^{-8}	1.07934×10^{-5}	Limestone/Sandstone
VESWAS4	284	-	47.3	47.33	0.023431	6.80565×10^{-3}	0.17695×10^{-5}	Limestone/Sandstone
VESWAS5	1482	43.4	48.6	48.6	0.014075	1.24936×10^{-6}	5.42221×10^{-5}	Limestone/Sandstone
VESWAS6	1344	-	20	20	0.007166	3.37444×10^{-6}	8.77354×10^{-5}	Saturated Sandstone
VESWAS7	2196	-	43.4	43.4	0.011517	7.31249×10^{-6}	1.90125×10^{-5}	Sandstone
VESWAS8	2307	-	47.8	47.8	0.011716	3.28834×10^{-6}	8.54969×10^{-5}	Saturated Sandstone
VESWAS9	2323	35.6	44.8	44.8	0.010594	2.93053×10^{-9}	7.61938×10^{-5}	Saturated Sandstone
VESWAS10	1066	31.4	36.2	36.2	0.017193	2.49738×10^{-5}	7.84179×10^{-5}	Sandstone
VESWAS11	1174	24.1	26.3	26.3	0.011643	1.14757×10^{-5}	2.76564×10^{-5}	Sandstone
VESWAS12	1138	22.8	27.5	27.5	0.012272	1.48683×10^{-5}	3.38996×10^{-5}	Sandstone
VESWAS13	1045	30.9	35.4	35.4	0.016804	2.90503×10^{-5}	8.97654×10^{-5}	Sandstone
VESWAS14	778	-	35.3	35.3	0.016714	1.98627×10^{-4}	6.13758×10^{-5}	Sandstone
VESWAS15	1604	14.4	25.3	10.9	0.009520	5.19042×10^{-7}	7.47421×10^{-5}	Sandstone
VESWAS16	1006	40.3	58.7	18.5	0.013138	3.84681×10^{-5}	1.55026×10^{-5}	Sandstone
VESWAS17	1197	40.2	60.5	20.3	0.017463	9.72431×10^{-6}	3.90917×10^{-5}	Sandstone
VESWAS18	1999	21.5	31.5	9.95	0.009003	3.02043×10^{-6}	6.49392×10^{-5}	Sandstone
VESWAS19	2473	-	69.1	69.1	0.016985	9.95196×10^{-10}	2.58751×10^{-5}	Saturated Sandstone
VESWAS20	1800	21.9	31	9.07	0.009102	1.26569×10^{-7}	2.77185×10^{-5}	Sandstone
VESWAS21	2132	26.8	36.2	9.4	0.009552	1.15928×10^{-8}	3.10687×10^{-5}	Saturated Sandstone
VESWAS22	1159	48.7	55.3	6.6	0.024882	1.25943×10^{-5}	6.13344×10^{-5}	Sandstone
VESWAS23	1276	50.6	55.0	4.4	0.022751	5.38829×10^{-6}	2.72648×10^{-5}	Sandstone
VESWAS24	1483	63.5	67.6	4.1	0.025366	1.24039×10^{-6}	7.87650×10^{-5}	Sandstone
VESWAS25	1629	42.5	23.2	13.0	0.95829	4.33540×10^{-7}	1.84255×10^{-5}	Sandstone

Table 2: Results of Statistical Analysis of Aquifer Parameters of Wasinmi

Aquifer Parameters	Min	Max	Range	Mean	Standard Deviation	Variance	Skewness \pmSE	Kurtosis \pmSE
Top Soil Resistivity (Ωm)	81.20	645.00	563.80	172.33	122.11	14911.05	2.78 \pm 0.46	1.33 \pm 0.90
Aquifer Resistivity (Ωm)	284.00	2473.00	2189.00	1513.8	536.32	287635.5	-0.021 \pm 0.46	-0.65 \pm 0.90
Aquifer Thickness (m)	14.40	63.50	49.10	32.25	11.16	124.63	1.03 \pm 0.46	2.80 \pm 0.90
Overburden Thickness (m)	4.10	69.10	65.00	27.73	17.42	303.29	0.43 \pm 0.46	1.43 \pm 0.90
Bedrock Resistivity (Ωm)	2.65	2695.00	2692.35	737.93	847.56	718353.2	1.19 \pm 0.46	-0.65 \pm 0.90
Bedrock Relief (m)	12.90	102.20	89.30	50.43	19.62	384.85	0.66 \pm 0.46	1.43 \pm 0.90
Longitudinal Conductance (S)	0.01	0.05	0.04	0.02	0.0087	0.000	2.43 \pm 0.46	-0.96 \pm 0.90
Coefficient of Anisotropy	1.00	1.00	0.00	1.0000	0.00005	0.000	-1.04 \pm 0.46	9.64 \pm 0.90
Transmissivity (m^2/s)	0.000002	0.00009	0.00009	0.00002	0.00003	0.000	0.24 \pm 0.46	-0.34 \pm 0.90
Hydraulic Conductivity (m/s)	0.00001	0.01	0.01	0.0003	0.0014	0.000	4.99 \pm 0.46	-1.59 \pm 0.90

Contour mapping

Contouring or Contour mapping is one of the techniques that can be used for interpretation of resistivity data (Ishola et al., 2016). Hydrological characterization and distribution of groundwater potentials of the study area was contoured using a computer software, "Golden Surfer 10" and 6 different types of contour maps were prepared for this study (Figure. 7.1- Figure. 7.6).

Aquifer resistivity Map

The resistivity contour map (Figure. 7.1) depicted the spatial distribution of resistivity across the study areas, thereby showing the ranking level of groundwater potential zones at each VES station (Ishola et al., 2016). Low to moderate and high resistivity values ranging between 284 Ωm and 2473 Ωm were identified. VESWAS4 and VESWAS14 have much higher groundwater potential values since the layer resistivity

falls below 1000 Ωm . This variation is evidently seen in the central ridges and steeply dipping slopes in the North West and South West of the map. The larger portion of the area have resistivity values far greater than 1000 Ωm typically seen in VESWAS7, VESWAS8, VESWAS9, VESWAS19 and VESWAS21, the highest being VESWAS 19. These areas are of higher resistivity values and thus have lower groundwater potentials. In the 3D map, there are five visible peaks which correspond to the areas with higher resistivity values in 2D (Figure. 7.1). These areas are sandstone/saturated sandstone, lithified sandstone underlain by clayey sand sometimes limestones characterized by good hydrogeological history which serves as the overlaying rock for groundwater accumulation, if weathered.

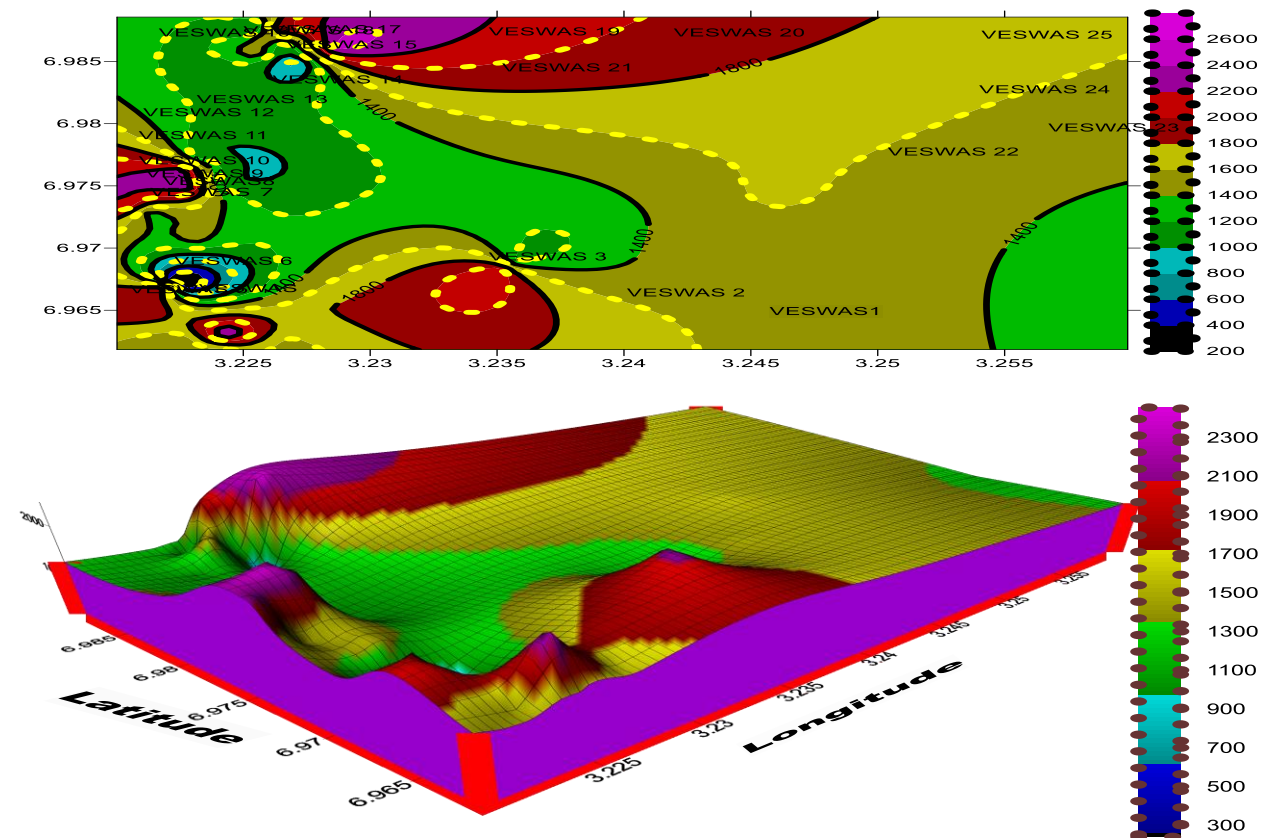


Figure 7.1: 2D/3D -View of Aquifer Resistivity Map of Wasinmi

Aquifer Unit(s) Thickness Map

The Aquifer thickness map (Figure. 7.2) showed various thicknesses of all locations sounded and also envisaged the reserve capacity of the hydrogeological structure within the area. Region of possible fractures/deep-seated faults are depicted by widely spaced closed contour lines, showing the vertical lateral distribution of the groundwater capacities within the study areas. Aquifer

thickness map can be used in ranking the waterbearing hydrogeological formation in terms of storage and conduit functions because volume of water from each VES station is a function of aquifer thickness which in turn reveals the various types of aquifer found in relation to groundwater accumulation as well as the degree of recharging. Thus, prediction can be made on thickness contrast alongside with aquifer resistivity

layer map considered earlier. The entire study area can be classified as good to moderate groundwater potential zones in terms of aquifer unit thickness distribution in the area (Ishola *et al.*, 2016). The highest recorded aquifer thickness value was 63.5m at VESWAS24 and the lowest value of 14.4m was at VESWAS15. The more productive water bearing zones categorized as potential zones occur at NE and SE parts of the investigated area (VESWAS22, VESWAS23,

VESWAS24 and VESWAS25) while the most prolific water-bearing reservoir is VESWAS24 with a conspicuous and pronounced dome structure displayed by the 3D map (Figure 7.2). A moderate groundwater potential zone with aquifer thickness ranging from 10m to 20m are found in VESWAS2 and VESWAS15 while the remaining parts of the study area were delineated as moderately saturated zone with less pronounced depression shown by the 3D map (Figure 7.2).

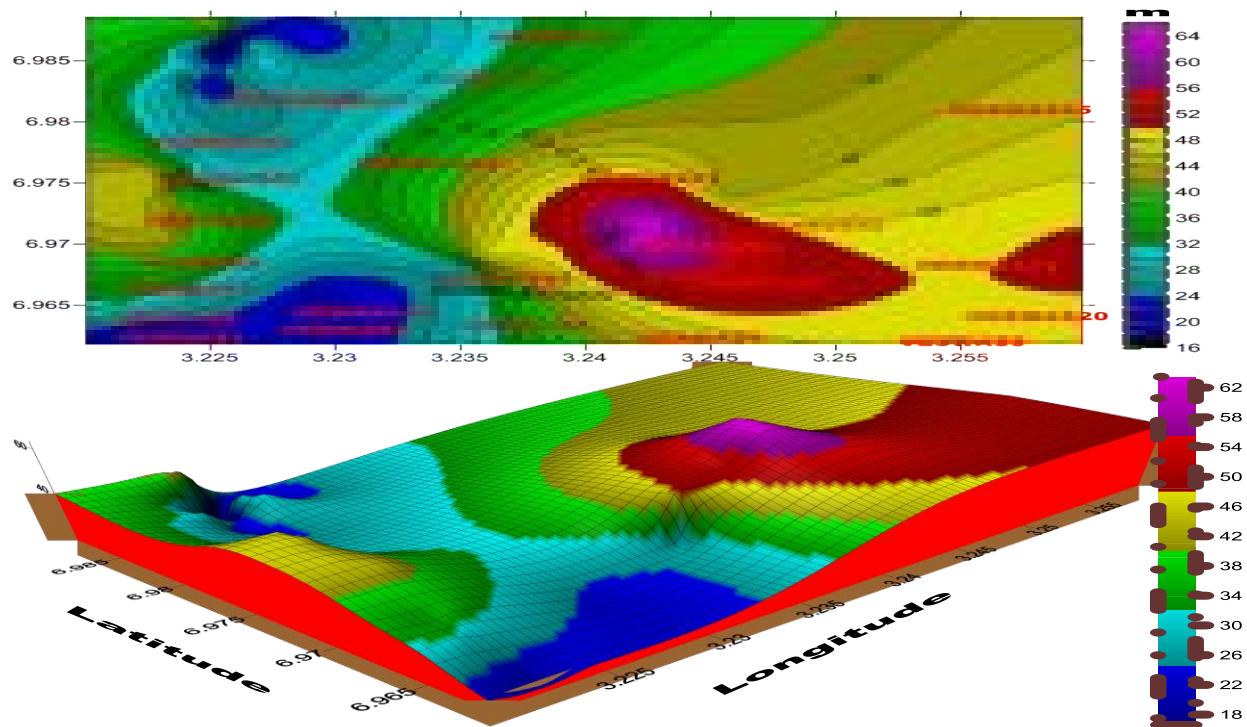


Figure. 7.2: 2D/3D -View of Aquifer Thickness Map of Wasinmi

Overburden Thickness Map

The term overburden refers to all formative/materials overlying the bedrock. The overburden thickness map revealed the overburden/depression along different sections which depicts clearly the depth to the fresh aquiferous zone. The areas of thick overburden are indicated by dense contour closures. The overburden thickness can be used to evaluate the drilling cost effectiveness in the area by the drilling contractor (Coker *et al.*, 2009; (Ishola *et al.*, 2016). Using the VES data, the overburden thickness was estimated at each data point. Values were interpolated and gridded using minimum curvature method over the investigated area to represent the overburden thickness map (Figure. 7.3).

The overburden thickness to basement is greatest at VESWAS19 which is located at the extreme west of the the map with a conspicuous and pronounced 'shoot-out', it also embraces VESWAS4, VESWAS5 and VESWAS8 with considerably high overburden

thickness values of 47.3 m, 48.6 m, and 47.8 m respectively while the areas with thinnest overburden is observed in VESWAS24 (4.1 m). Areas with VES stations whose overburden thickness values are greater than 26.0m are considered to be of better groundwater potentials than other areas with lower overburden thickness values. In this area, larger portion of the locations in the North and South-West section of the map have their overburden thickness greater than 26 m while some of the sizeable portions of the locations in South-East section of the map have their overburden thickness less than 26 m; these are VESWAS6 (20 m), VESWAS15 (10.9 m), VESWAS16 (18.5), VESWAS18 (9.95), VESWAS20 (9.07), VESWAS21 (9.4), VESWAS22 (6.6), VESWAS23 (4.4), VESWAS24 (4.1) and VESWAS25 (13 m). The locations with overburden thickness values between 1 m and 10 m above are considered as low/thin overburden thickness.

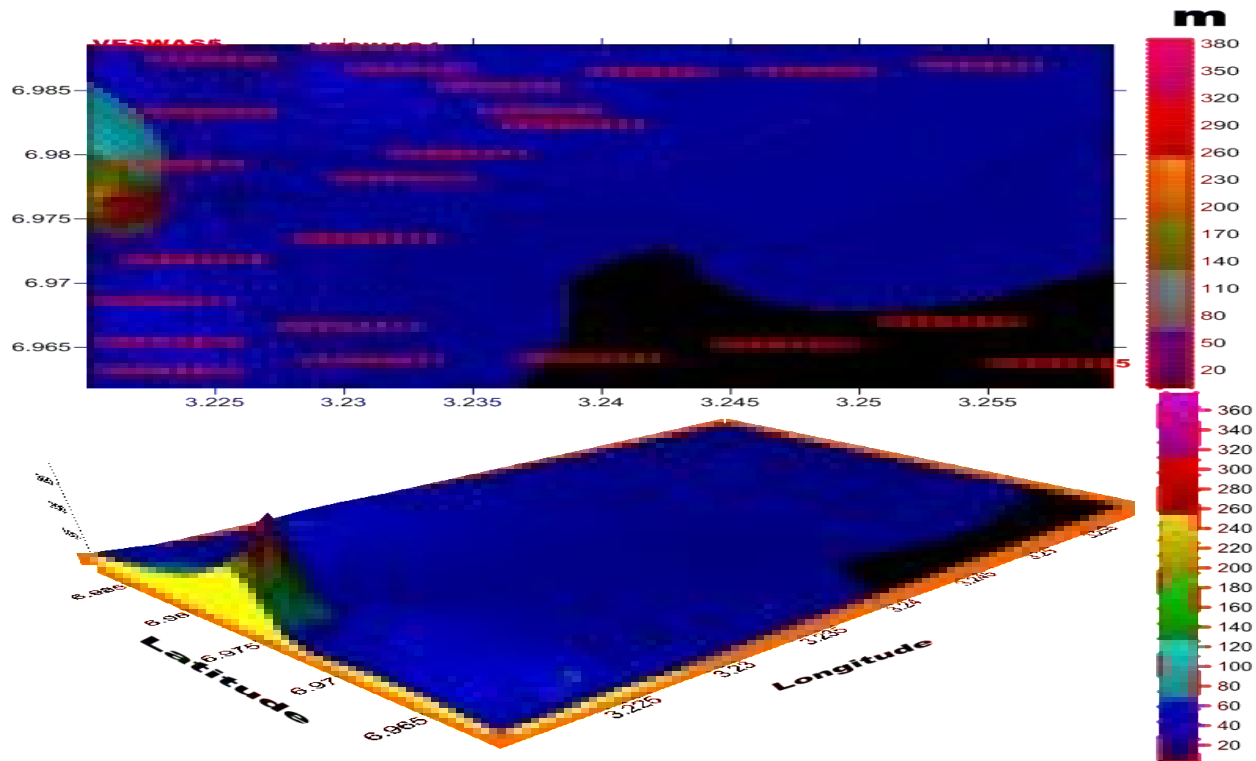


Figure. 7.3: 2D/3D -View of Overburden Thickness Map of Wasinmi

Longitudinal Unit Conductance Map

Considering a prism of aquifer material showing unit square cross-sectional area A , thickness h , the total longitudinal conductance S can be calculated for each VES station from the interpreted VES data.

The longitudinal conductance of each subsurface layer S_i , can be determined for each VES site from the interpreted VES data; this gives the total longitudinal conductance S , using equation 4 (Onuoha and Mbazi, 1988).

$$S_i = \sum_{i=1}^n \frac{h_i}{\rho_i} \quad i = 1,2,3,4 \quad (4)$$

The qualitative use of this parameter is to demarcate changes in total thickness of low resistivity formation. Higher variation in conductance values were observed at different sections of the map but decreases towards the Southern part of the map (Figure 7.4). Based on the reciprocal relationship of resistance and conductance, $\sigma = \frac{1}{\rho}$, the more a geological formation is conductive, the less it is resistive indicating a permeable formation (Makinde *et al.*, 2016). As the conductance increases the resistivity naturally decreases pointing towards

groundwater potential aquifer (Gowd, 2004). Furthermore, the map of longitudinal conductance reveals the visual illustration of the protective capacity of the overburden layer. In the locations with values of $S > 1.0$ Siemens would indicate zones in which the confined aquifer would be protected should the geophysical survey permits lithological identification and characterization of the conditions of the underground groundwater flow of the study areas. Also, the map of longitudinal conductance illustrates the impermeability of the confining clay layer. Areas with values of $S > 1.0$ Siemens would indicate zones in which the confined aquifer would be protected, while in comparison, values of $S < 1.0$ Siemens would indicate zones of probable risks to contaminant seepages.

In all the locations investigated in the study area, the longitudinal unit conductance is less than unity ($S < 1.0$ Siemens) which showed that the study areas could be prone to external invasions thereby hampering the sanitary quality of the aquiferous zones in the study areas.

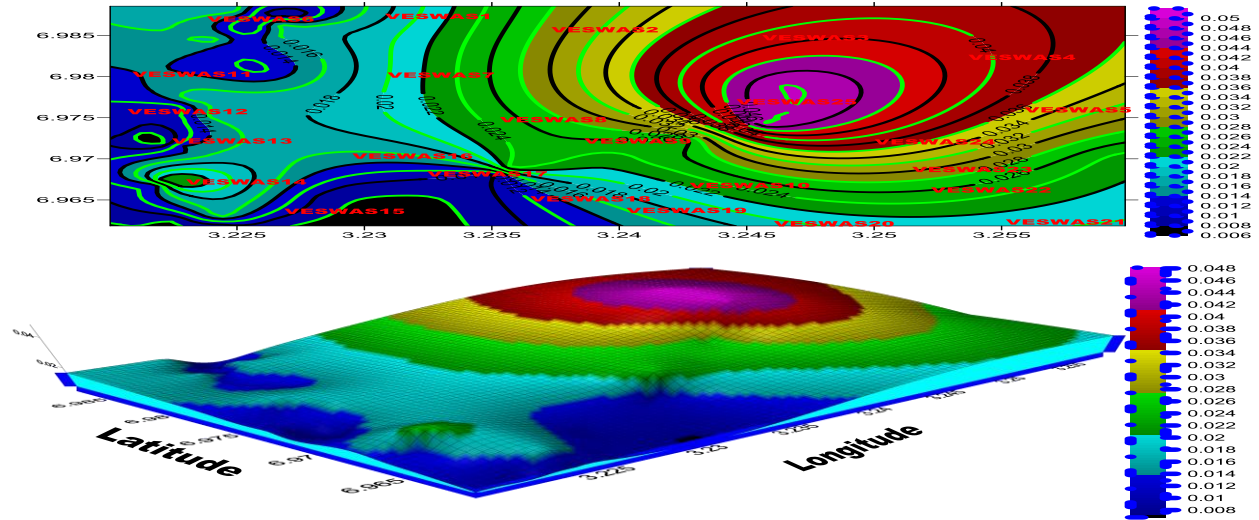


Figure 7.4: 2D/3D – View of Longitudinance Conductance Map of Wasinmi

Hydraulic Conductivity Map

The hydraulic conductivity K is obtained using the relation $T = Kh$ where T is the aquifer transmissivity and h is the aquifer thickness. Based on the Darcy’s law and ohm’s law, Niwas and Singal, (1981) have derived the following relations for the modeling of the groundwater resources of an area.

$$T_r = K\sigma T = \frac{KT}{\rho} = 1 \tag{5}$$

where T_r is the transverse unit resistance and $\sigma = \frac{1}{\rho}$ is the electrical conductivity

$$KT = \rho \tag{6}$$

$$\text{Therefore, } K = \frac{\rho}{T} \tag{7}$$

Small variation in hydraulic conductivity is widely observed in most sounding locations in this study area except VESWAS4 with the highest hydraulic value of 6.80565×10^{-3} m/s displaying a conspicuous prominent peak having a small area of spread as shown in the 3D map (Figure. 7.5). VESWAS10 has the lowest hydraulic conductivity value of 9.95196×10^{-10} m/s.

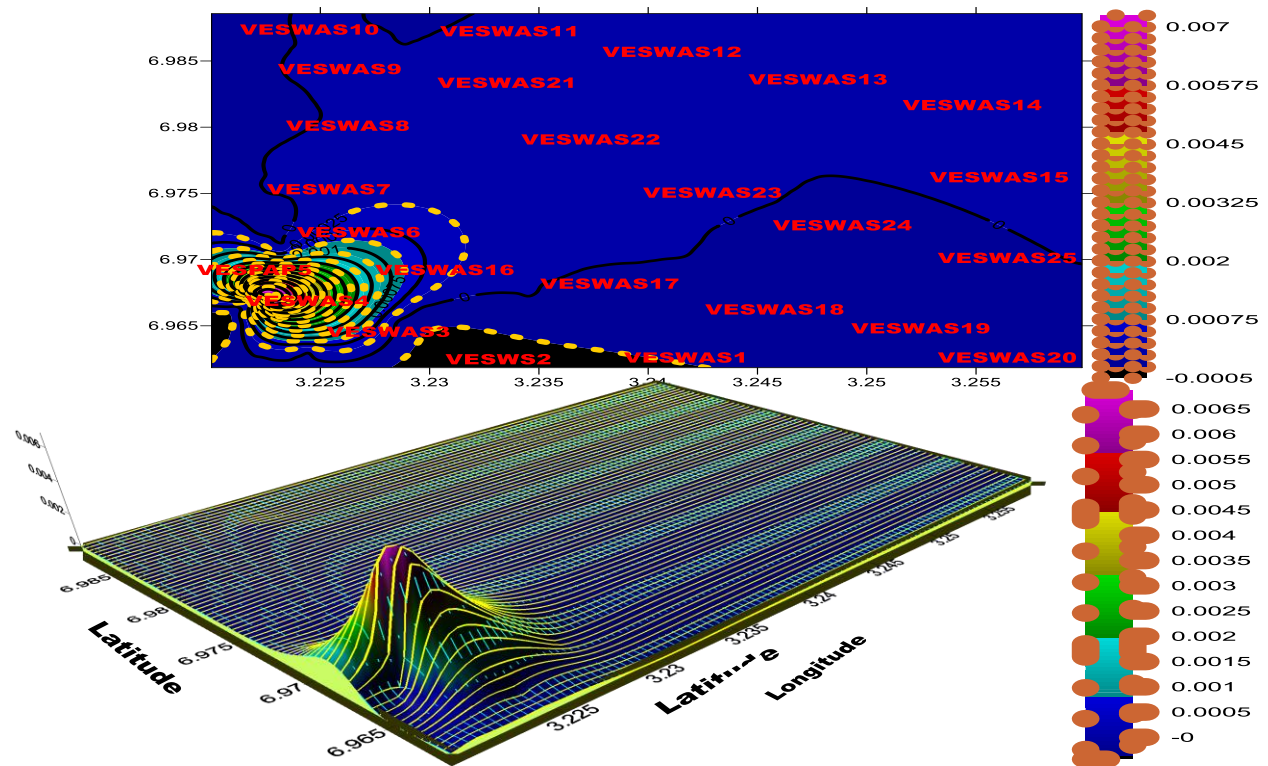


Figure 7.5: 2D/3D – View of Hydraulic Conductivity Map of Wasinmi

Transmissivity Map

This map illustrates the variation in the rate of flow of groundwater within the aquiferous zones under a unit hydraulic gradient in the respective locations in the study area. Thus, transmissivity is directly proportional to hydraulic gradient using the equation

$$T = Kh. \quad (8)$$

Very low transmissivity values are recorded in almost all the study areas with lowest transmissivity value of $0.17695 \times 10^{-5} \text{ m}^2/\text{s}$ in VESWAS4 and the highest

recorded value is observed in VESWAS13 ($8.97654 \times 10^{-5} \text{ m}^2/\text{s}$) which embraces VESWAS6 and VESWAS8 with the value of $8.77354 \text{ m}^2/\text{s}$ and $8.54969 \text{ m}^2/\text{s}$ respectively. In the 3D map, places of higher resistivity values are seen with rising or bulging show at different parts of the map while fairly low or very low locations are displayed as plain or slight depression at the other sections of the map (Figure. 7.6).

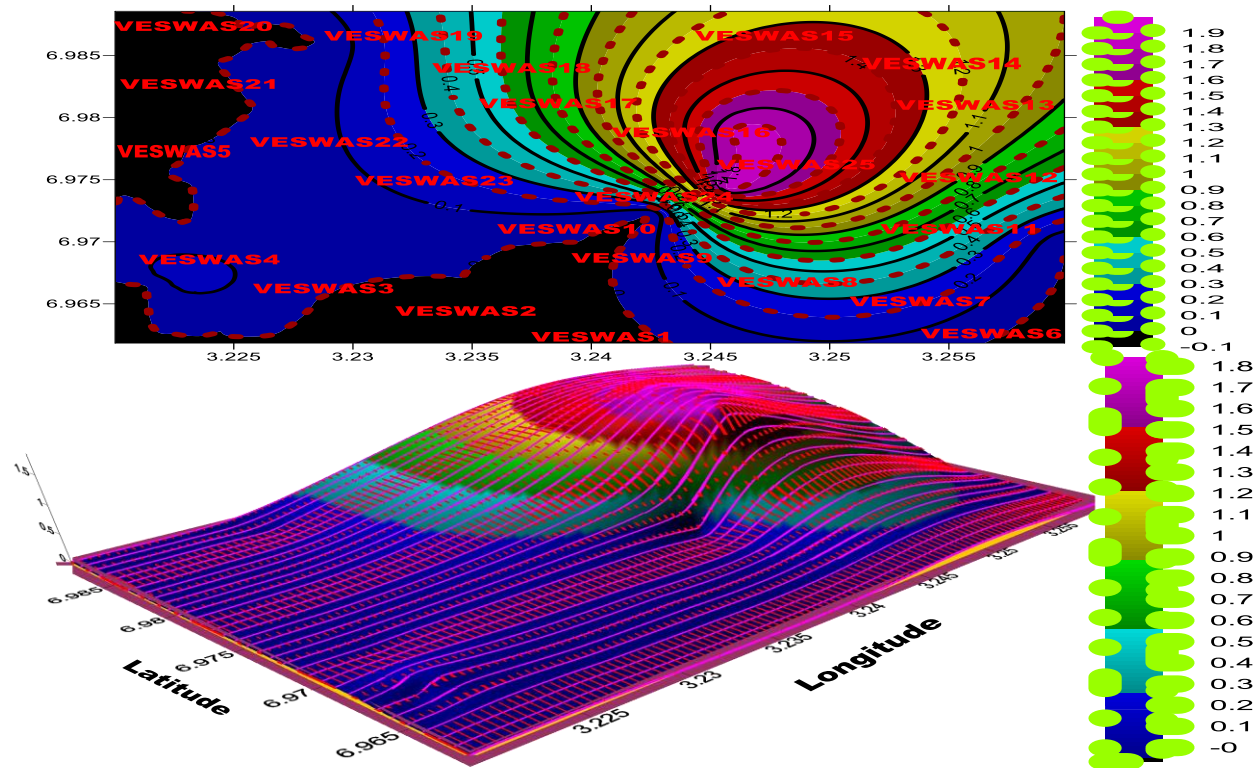


Figure 7.6: 2D/3D – View of Transmissivity Map of Wasinmi

CONCLUSION

It is observed from this results that areas where there were high resistivities turns out to be areas where we have low transmissivity values and vice versa. This is seen in VESWAS19, VESWAS9 and VESWAS21 (Higher resistivity with lower transmissivity) and VESWAS13, VESWAS4 and VESWAS14 (Lower resistivity with higher transmissivity.) In VESWAS9 and VESWAS10, though the resistivity value is high, yet the transmissivity is relatively high. This is due to the high value of aquifer thickness in their aquifer units. In the upper north east area of the study map, where we have VESWAS25 and VESWAS6, there are relatively shallower aquifers when compared to the other VES points in the study area. VESWAS6 has the shallowest depth to aquifer, which is at about 20 m. The aquifer which is inferred to be a perched aquifer is relatively small when compared to other aquifer units in the study area. The underlying layers of the aquifer unit include sandstone and a thick sandy clay layer (Figure 4). Deep aquifers are in VES points VESWAS3, VESWAS4, VESWAS5, VESWAS7, VESWAS8, VESWAS9 and VESWAS21 and deeper aquifers are found in VES points VESWAS16, VESWAS17, VESWAS19, VESWAS22, VESWAS23 and VESWAS24.

Aquifer thickness in the study area varies from 14.4 m to 63.5 m. The smallest aquifer thickness is in

VESWAS15 where we have the inferred perched aquifer.

The depth to aquifer is about 63.5 m, which is shallower compared to VESWAS19. VESWAS23 also has a high aquifer thickness of about 50.6 m with a depth to aquifer of about 55.0 m. VESWAS22 has an aquifer thickness of about 48.7 m and a depth to aquifer of about 55.3 m. Boreholes drilled in VES points of VESWAS23 and VESWAS24 will be capable of serving the inhabitants of Central and Southeastern part of the study area and VES points of VESWAS16 and VESWAS17 can serve the inhabitants of the Central and Northwestern and Southern part of the study area respectively. Other boreholes can be drilled in VES points of VESWAS9, VESWAS10, VESWAS20, VESWAS21, VESWAS22 and VESWAS25 to support the aquifers at VES point VESWAS16, VESWAS17, VESWAS23 and VESWAS24 for maximum supply of groundwater in the entire study area. Further groundwater development through borehole construction in the study area must be preceded by a detailed geophysical investigation (VES) with at least current electrode spacing of about 600 m to 800 m. This is to clearly determine the thicknesses of the wide spread shale/clay sand in the area. The boreholes must be logged to determine the exact screen position(s). This will minimize the problems associated with the occurrence and distribution of groundwater in the area.

REFERENCES

- Adegoke O.S (1969). Eocene Stratigraphy of Southern Nigeria. Extract Dememries Du Bureau Durecherdedseologique Min 67: 23-40.
- Alile, O. M. and Amadasun, C.V.O (2008). Direct Current probing of the subsurface Earth for Water Bearing Layer in Oredo Local Government Area, Edo State, Nigeria. *Nigeria Journal of Applied Science*, Vol. 25: 107-116.
- Alile, O. M, Ujuambi., and Evbuomwan, I.A., (2011). Geoelectric investigation of groundwater in Obaretin-Iyanonon Locality, Edo State, Nigeria, *Journal of Geology and Mining Research*, 3(1), pp 13-20,
- Archibong, E.E (1978). The stratigraphy of Ojo-1 borehole, Department of Geology, University of Ife, Nigeria 43 pp
- Ariyo, S.O, Adeyemi G.O., and Oyebamiji A.O. (2009). Electromagnetic VLF Survey for Groundwater Development in a Contact Terrain; a Case Study of Ishara-Remo, Southwestern Nigeria. *Journal of Applied Sciences Research*, 5(9): 1239-1246, 2009 © 2009, INSInet Publication.
- Bobachev, A., (2002). IPI2win- A window software of an automatic interpretation of resistivity sounding data; Moscow State University.
- Coker, J.O; Makinde, V. and Olowofela, J.A. (2009). Geoelectric Sections with available Borehole Nigeria *Journal of sciences*; Vol. 32pp 105-111.
- Dobrin, M. B., (1985). Introduction to geophysical prospecting (4th edition). Mc.Graw Hill Inc. New York, USA p. 629.
- Ekwe, A. C., Onu, N. N., Onuoha, K.M., (2006). Estimation of aquifer hydraulic characteristics from electrical soundings data, The case of middle imo river basin aquifer, Southeastern Nig., *Journal of Spatial hydrogeology*.
- Goes, B. J. M and Meekes, J. A. C (2004). An effective electrode configuration for the detection of DNAPLs with electrical resistivity tomography. *J Environ Eng Geopys* 9:127–141 [CrossRefGoogle Scholar](#)
- Gowd, S. S (2004). Electrical Resistivity Surveys to delineate Groundwater Potential Aquifers in Peddavanka Watershed, Anantapur District, Andhra Pradesh, India. *J. Envir. Geol.*, 46: 118-131.
- Ishola, S.A., Makinde, V., Aina, J.O., Ayedun H., Akinboro F.G., Okeyode I.C., Coker J.O., and Alatise O.O (2016). Aquifer Protection Studies and Groundwater Vulnerability in Abeokuta South Local Government Area, South-West Nigeria, *Journal of Nigerian Association of Mathematical Physics*, Vol 33,(January, 2016), pp 347-362 © J.of NAMP
- Ishola S.A (2019). Characterization of Groundwater Resource Potentials using Integrated Techniques in Selected Communities within Ewekoro Local Government Area South-West Nigeria. Ph.D Thesis
- Jones, H.A and Hockey, R.D (1964). The Geology of Parts of Southwestern Nigeria. *Geol Survey Nig. Bull.* 31: 22 – 24.
- Keary, P., and Brooks M. (1991). An Introduction to Geophysical Exploration (2nd Edition). Oxford, Blackwell, .Blackwell Scientific Publications, London. pp. 254.
- Kehinde-Phillips, T. Ogun State maps, In: Onakomaya, S.O., K. Oyesiku and Jegede, (1992). Ogun State in Maps. Rex Charles Publishers, Ibadan, pp: 187 Rex-Ibadan,
- Koefoed, O. (1979). Geo-sounding Principles I, Resistivity sounding measurements. Elsevier. Oxford.
- Kogbe C.A (1976). The Cretaceous and Paleogene sediments of southern Nigeria. In C. A. Kogbe (Ed.) *Geology of Nigeria*. pp. 325- 334.
- Makinde V. , Ishola, S.A Akinboro, F.G , Okeyode, I.C. Agwuegbo, S.O.N. Ozebo, V.C. Coker, J.O and Aina, J.O. (2016). Evaluation and Analysis of Geoelectric Parameters of Abeokuta South Local Government Area, Ogun State, South West Nigeria. *Journal of Nigerian Association of Mathematical Physics* (2016), Volume 35 (May 2016) Pp 275-286. www.nampjournals.org; www.tnamp.org
- Mamah L. I. and Eze, L. C. (1988). Electromagnetic and ground Magnetic Survey over Zones of Lead-Zinc Mineralization in Wanakom (Cross River State). *Journal of African Earth Sciences*, Vol. 7, No.5-6, pp. 749-758.
- Niwas C and Singal, D. (1981). Transverse unit Resistance modeling of the Groundwater Resources of an area. Vol 2 (11)
- Nur, A., and Kujir, A. S., (2006). Hydro-geo-electrical study in the Northeastern Part of Adamawa State, Nigeria. *Journal of Environmental Hydrology* Vol. 14. pp1- 7.

- Offodile, M. E. (1983). The occurrence and exploitation of groundwater: in Nigerian Basement rocks. Nigeria Jour of Min and Geology, Vol. 20 Nos. 1 and 2 pp. 131–146.
- Ogbe, F.G.A. (1972). Stratigraphy of Strata Exposed In the Ewekoro Quarry, Western Nigeria. In African Geology TFJ Dessauvage & Whiteman Eds, University Press, Nigeria, pp. 305–322.
- Okereke, C. S., Esu O.E., and Edet, A. E., (1998). Determination of potential groundwater sites using geological and geophysical techniques in cross river state, Southeastern Nigeria;
- Okosun, E.A. (1998). Review of the early Tertiary stratigraphy of southwestern Nigeria, Jour. Min. and Geol. Vol. 34, no 1, pp. 27–35.
- Okwueze, E. E., (1996). Preliminary findings of the groundwater resource potentials from a regional geoelectric survey of the Obudu basement area, Nig. Global journal of pure and applied sciences, 2(2), pp 201-211.
- Oladeji, B.O (1992). Environmental Analysis of Ewekoro Formation At The Shagamu Quarry. Nig. J. Min. Geo. 28(2): 148-156
- Olayinka, A. I., (1990). Electromagnetic profiling for groundwater in Precambrian Basement Complex areas of Nigeria: Nordic Hydrogeology, Vol. 21 pp. 205 – 216.
- Omatsola, M. E, Adegoke, O. S (1981). Tectonic Evaluation and cretaceous stratigraphy of the Dahomey Basin, J. Min. Geol. 5(2): 78-83.
- Onuoha, K. M and Mbazi, F. C. C (1988). Aquifer Transmissivity from Electrical Sounding Data. In the Case Study of Ajali Sandstone Aquifers, Southeast Of Nigeria, Vieweg-Verlag, Pp 17-30
- Parasins, D. S. (1986). Principles of Applied Geophysics. Chapm & Hall U.S.A. pp. 402.
- Reyment, R. A. (1965). Aspects of the Geology of Nigeria: U.I Press. pp. 36 – 43.
- Singh, K. P., (2005). Non-linear estimation of aquifer parameters from surficial resistivity measurements: Hydrogeology and Earth System Sciences Discussions (HESSD) 2, pp 919-938.
- Ushie, F., Harry, T., and Affiah, U. (2014). Reserve Estimation from Geoelectrical Sounding of the Ewekoro Limestone at Papalanto, Ogun State, Nigeria. Journal of Energy Technologies and Policy ISSN 2224-3232 ISSN 2225-0573 (Online) Vol.4, No.5, pp 28